STUDY THE INFLUENCE OF PRECIPITATE SIZE DISTRIBUTION ON HARDNESS OF ALUMINIUM 6063 ALLOY UNDER CONSTANT AGING TEMPERATURE

L.W.U.R. Dilrukshi

188079K

Degree of Master of Science

Department of Materials Science and Engineering

University of Moratuwa,

Sri Lanka

June 2021

STUDY THE INFLUENCE OF PRECIPITATE SIZE DISTRIBUTION ON HARDNESS OF ALUMINIUM 6063 ALLOY UNDER CONSTANT AGING TEMPERATURE

L.W.U.R. Dilrukshi

188079K

Thesis/Dissertation Submitted in Partial Fulfillment of the Requirements for

The Degree Master of Science

Department of Materials Science and Engineering

University of Moratuwa,

Sri Lanka

June 2021

DECLARATION

I declare that this is my own work, and this thesis does not incorporate without the acknowledgement of any material previously submitted for a Degree or Diploma in any other University or Institute of higher learning to the best of my knowledge and believe it does not contain any material previously published or written by another person except where the acknowledgement is made in the text.

I hereby grant to The University of Moratuwa the irrevocable, non-exclusive, and royalty free license to archive and make my work accessible in whole or in part in all forms of media, now or hereafter known. I agree that the document mentioned above may be made available immediately for worldwide access unless an embargo applies.

I retain all other ownership rights to the copyright of my work. I also retain the right to use in future works (such as articles or books) all or part of my work. I understand that I am free to register the copyright to my work.

Signature: *UOM Verified Signature* Date: 2021.06.02

The above candidate has carried out research for the MSc. thesis under my supervision.

Signature of the supervisor: *UOM Verified Signature* Date: 2021.06.02

Name of the Supervisor: Dr. G.I.P.De Silva

ACKNOWLEDGEMENT

First of all, I would like to thank my Supervisor Dr. G.I.P. De Silva, Senior Lecturer (Grade 1) at the Department of Materials Science and Engineering, University of Moratuwa. He has made available his support in a number of ways since beginning of the research to the very end. He had guided me and formed me to complete my research successfully by his huge scientific knowledge with industrial experience. I would like to thank, Prof.M. Narayana, Department of Chemical and Process Engineering, University of Moratuwa for giving the fullest support in this work.

My sincere thank should also go to the research committee for directing me to the right way till the end. I greatly appreciate the assistance that I received from the head of the department and the academic and nonacademic staff of Department of Materials Science and Engineering, University of Moratuwa.

Further, extend thanks to the Senate Research Council (SRC) grant - SRC/LT/2018/27, of University of Moratuwa for their financial assistance. I would also like to extend my gratitude to the Alumex (Pvt) Ltd for providing samples and technical assistance in making this research work a success.

The outcome of this thesis is a collection of efforts. There are lot of helpful hands behind its success. I would like to express my gratitude to my parents, husband and all the family members for giving me the strength not only to achieve this goal, but for being with me throughout the entire way of personal, educational and career lives. Your support guided me to climb up the ladder.

Last but not least, I would like to express my warm hearted thanks to my colleagues, relatives and everyone who has supported me in every way to make the MSc. thesis a success.

ABSTRACT

The improvement of mechanical properties of heat-treated (T6) Aluminium 6063 alloy is caused due to hindrance of the dislocation line by the precipitates which is formed during the heat treatment process. The perception of the inter-relation between microstructural variations and mechanical properties with process parameters is essential, as it facilitates the optimization of the processing routes of the industry to be profitable. Several combinations regarding the relationship between properties and process parameters developed in previous studies without considering the precipitate size distributions. The current research focuses on finding the influence of age hardening process parameters on the precipitate size distribution and its effect on the hardness of the final product.

Prepared samples were solution treated and quenched in water, followed by aging treatments for different periods. The Scanning Electron Microscope (SEM)/ Energy Dispersive Spectroscopy (EDS) analysis of precipitates was used to identify the Fe-Si-rich and Fe-Si-Mg-rich precipitates/β phase in the matrix (α phase). Further analysis of precipitates was done through IMAGE J software and MS EXCEL. The change of precipitate size distribution with different soaking times and its effect on the hardness of the Alloy was studied. A significant decrease in hardness was witnessed when the particles coarsen above 1.5 μm, for the aging time beyond 270 min at 190^0C.

Keywords: *Al 6063, Age hardening, Hardness, Precipitate size distribution*

TABLE OF CONTENT

LIST OF TABLES

LIST OF FIGURES

LIST OF ABBREVIATIONS

IMAGE J	Java-based image processing program
EHT	Event Horizon Telescope
HB	Brinell Hardness
EDX	Energy Dispersive X-Ray
TTP	Time Temperature Property

CHAPTER 01

1. INTRODUCTION

Among other Al-Mg-Si alloys, Al 6063 alloy is the main structural material in use due to its comparatively excellent strength to weight ratio, corrosion resistance, and extrudability, which could play a vital role in the manufacturing of structural items such as bars of varying cross-sections, door and window frames, partitioning, and aircraft and automotive structures [1]. The Alloy consists of Mg (0.45-0.90 wt %) and Si (0.2-0.6 wt %) as its major alloying elements [2]. The presence of these alloying elements to form Mg_2Si in the range of 0.71 to 1.42 (wt.%) [3] influences the mechanical properties of the Alloy. The optimum solute level and production process parameters should be applied to accomplish excellent mechanical properties, [4] and the formation of uniformly dispersed particles of a second phase within the matrix causes the Al 6063 alloy to obtain the required strength and hardness [5]. These precipitates act as obstacles to the dislocation glide and hinder the relative deformation while increasing the hardness. The dislocation glide passed through these impediments by shearing or bypassing is decided by the nature of the particles, size distribution, and inter-particle spacing [6].

These precipitates/particles are attained by a process called artificial aging. The Alloy, which is formed immediately from the solution treatment, is rich in solute atoms and vacancies, causing a thermodynamically unstable structure and gains a metallurgical driving force to move to the equilibrium stage [7]. If the Alloy is exposed to room temperature for a more extended period, it gets hardened slowly, and this process is called natural aging [8]. The overall effect of natural aging is not in favor of the mechanical properties and production process. The solution-treated samples are stored in a deep freezer right away to prevent natural aging until the artificial aging is started [5].

The elastic stress in the matrix around the precipitates is formed since the early stage of precipitates due to relative size differences of the atoms. Magnesium atom is about 10% larger relative to the Al atom. Silicon atom is smaller than an Al atom roughly by 21%. When considering the GP (Guinier-Preston) zones formed in the Alloy, the

ones consisting of hexagonal structure parallel to the <100> direction gained coherence with the matrix. But structure perpendicular to the central axis has a cylindrical interface formed non-coherent with the matrix the overall effect results in semi-coherent properties at last [7][8]. At the beginning of the process, the number and size of precipitate increase with aging time at a particular aging temperature. The increment in metal hardening would occur due to this behavior, and this effect is changed when the precipitate is reached its critical size [9]. Further increment of aging would reduce the number of precipitates while continuous increment of its size due to coarsening. The inter-particle space is increased, leading to the bowing and bypass mechanism with reduction of hardness.

According to the previous studies [6][7] "cutting through" mechanism significantly affects to increase the hardness, rather than the "bowing and bypassing." The degree of strengthening is determined by the particle size, size distribution as well as inter-particle spacing. In this work, all types of precipitates distributed in the matrix (solid solution) are considered the second phase and denoted as β. Researches [3][10][11] have shown that the "cutting through" mechanism becomes predominant within the particles in the size range of R_1(<0.2μm). The "bowing and bypassing" mechanism becomes predominant among the particles of R_2 (0.2-1.5 μm). Simultaneously, both mechanisms are activated within this range according to the size of the majority.

Research has been carried out regarding dislocation interaction with precipitate obstacles in age-hardened Al alloys through computational simulations [12]. For a given aging temperature, increasing the average radius of precipitates while maintaining a constant volume fraction would initially increase the strength to a maximum value and be followed by a diminishing in strength (over aging) [13]. This type of system follows Ostwald Ripening's behavior [14]. The larger particles (energetically favored) were grown further by dissolving small particles while minimizing the total area covered by precipitates. In 1958 Lifshitz and Slyozov derived a mathematical model for such a system to evaluate the particle radii distribution, which is presently known as LWS theory. After applying the aging treatment, mechanical properties depend on the size and size distribution of the precipitates being formed, which is determined by the processing time and

temperature [15]. As a significant structural material used in a range of industry applications, it is very worthwhile to identify the relationship of mechanical behavior (hardness) with precipitate size distribution (second phase) formed due to the aging treatment. If the manufacturer needs to meet any customized property, they must make several changes in the production line relatively the present condition, wasting time and money. The following research objectives are associated with finding a solution for this matter. The following work is focused on studying the variation of the hardness of Al 6063 alloy with the precipitate size distribution in different size ranges at 190^{o}C under several aging time.

1.1 Objectives of Research

- To study the effect of soaking time of age hardening treatment on precipitate size distribution.
- To study the influence of precipitate size distribution on hardness.

1.2 Outline of the Dissertation

Chapter 1: Discuss the prominence and requirement of this research based on real applications in industry and its contribution to improving its existing production process and quality.

Chapter 2: Consists of a comprehensive literature review focused on earlier research works to understand the alloy behavior with process bounds. Furthermore, under chapter 2, the precipitate identification and hardening mechanism, the theoretical background of precipitate nucleation and growth were discussed.

Chapter 3: Detailed explanation of the experiment program, Testing methods, Image J software, and its outcomes.

Chapter 4: In-depth discussion on test results and theoretical background of some specific production processes, microstructural evaluations, and precipitate identification for all heating profiles. Study of the graphical representation of precipitate size distribution and its effect on the hardening.

Chapter 5: Conclusions of the study.

Chapter 6: Suggestions for future works.

CHAPTER 02

2. LITERATURE REVIEW

Age hardening is a well-known process that can enhance the mechanical property by forming secondary phase particles within the Alloy matrix [16][17]. Experts conduct many experiments/research due to the importance of this process in the industry. The change in mechanical properties was studied by changing the process parameters, and attempts have been made to improve them further.

An intensive literature survey has been done to summarize the available knowledge of this Alloy, process parameters, and precipitates to determine the boundaries of the proposed work.

2.1 Age Hardening

A.Wilm discovered the age hardening of Aluminium alloy in 1906 by accident [7]. The metal was getting hardened with time (aged) when kept at room temperature after rapidly cooled from high temperature (around 550^0C). There were no detected structural changes in the optical microscope level [7]. Guinier and Preston first found evidence for the clustering of atoms (GP zones) in 1938 by x-ray scattering. Nicholson and Nutting did the microscopic observation of GP zones in 1950 by TEM. With the requirement coming from the industry, Al 6063 alloy was first produced in 1944 [2][18] [19].

2.1.1 Solution Heat Treatment Process

This makes a complete random solid solution of Mg and Si atoms in the aluminum matrix donated as α-phase. The amount of heat applied is an essential parameter at this stage. Enough heat should be supplied to the sample at A (Figure 2-1) for complete phase transformation.

In 1999, Rafiq A. Siddiqui et al. [20] studied the influence of aging parameters on the mechanical properties of the same metal. All their sample were solution treated at 520^oC for two hours. The samples were quenched in water at room temperature and

transferred to a freezer to avoid natural aging. Mechanical properties were measured after the successful completion of the process.

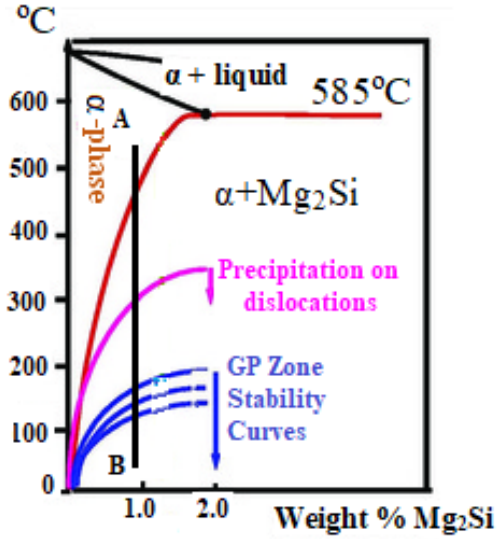

Figure 2-1: Al-Mg_2Si pseudo-binary section [7]

Jose Luis Cavazos et al. [15] have studied the sensitivity of a heat treatable aluminum alloy. They have selected Al 6063 alloy for the experiment. The samples were solubilized at 520°C for 4 hours. Different cooling rates were arranged after solution treatment and found its sensitivity for the final product after aging.

2.1.2 Quench in Water

At 530°C (Figure 2-1, point A), the microstructure consists of a random solid solution of magnesium and silica atoms in the aluminum matrix, denoted as α phase. In this research, samples were put four hours under this temperature because the system needs enough heat to create a solid solution. The solute atoms are getting moved faster due to the high vacancy concentration available at this moment. Although the system undergoes a prolonged cooling process, the microstructure at the room temperature would consist of a diluted concentration of solute atoms in the α phase together with an equilibrium second phase of Mg_2Si, which was formed at high temperature (between about 410°C ~ 300°C) according to the findings of Hong-Ying LI et al. [21]. Jose Luis and his team had concluded that the final hardness of Al 6063 alloy was influenced only by a cooling rate lower than 10°C/s after solution treatment [15].

This temperature range was explained in TTP (Time-temperature-property) curves of Al 6063 alloy, which the Hong-Ying Li group developed as in Figure 2-2.

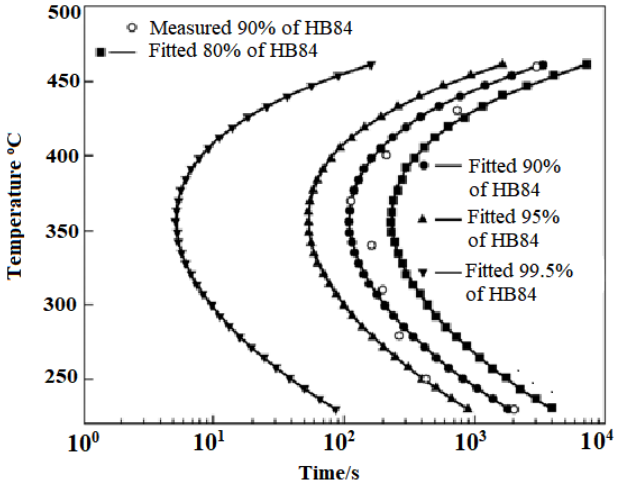

Figure 2-2: TTP curves of Al 6063 alloy [21]

When considering the intersection points of the 10s line and the TTP curve for 99.5% of the maximum property, approximate values for the critical temperature range are about 300ºC ~410ºC with a nose temperature of 360ºC. The rapid reduction in hardness of the product at the end was occurred due to the extension of isothermal time within this temperature range.

But when the system is cooled rapidly as it was water quenched, the situation becomes completely different. Suppose the metal is water quenched from A to B (Figure 2-1). In that case, the quenched Alloy is in a state of a supersaturated solid solution of high concentration of both solute atoms and vacancies with a metallurgical driving force.

2.1.3 Ageing Heat Treatment Process

The quenched Alloy is in a metastable state of supersaturated solid solution. Therefore, it is thermodynamically unstable and requires a high concentration of metallurgical driving force to move to the equilibrium structure. If the metal is kept at room temperature, the structure gets harder at a low rate because the process occurred inside with the effect of highly concentrated solute atoms and vacancy, called natural aging [7][8]. The samples were stored in a freezer [20] to avoid this process.

As explained above, heating the metal between 100ºC-200ºC for few hours gives the ability to accelerate the hardening process by forming precipitates (second phase particles) inside the aluminum matrix (α -phase) [19][20][22][23]. The second phase particles with several stages developed, during the aging process can be summarized as below.

GP zones ⟶ β" needles ⟶ β' rods ⟶ β Platelets (Mg_2Si) [24]

Aramide Fatai investigated the effect of aging temperature and soaking time at that particular temperature on the mechanical properties of Al 6063 alloy [22]. The best mechanical properties were obtained by the combination of aging at 225ºC for 3 hours through a testing range of temperatures with several time frames.

F. Ozturk et al. [1] had found the influence of aging parameters on the mechanical properties of Al 6061 alloy. The treatment was done at 200ºC for a range of keep time, and the results proved the adequate soaking time as 2 hours. The artificial aging behavior of Al 6063 alloy was investigated by M. A. Abdel-Rahman and his colleagues [25]. The aging was done under various temperatures for different soaking times to identify the best combination of mechanical properties. The ageing temperature of 170ºC for 8 hours was selected as the best combination of parameters.

2.2 Energy Conversion in Precipitate Formation

The precipitates are formed randomly within the matrix and this process is called homogeneous nucleation. The understand of free energy change associated with this cluster formation may happened is divided in to three categories such as new volume, new area between the solute cluster and matrix and size difference [7].

The creation of new volume V reduces the free energy by $V\Delta G_{v.}$ The free energy increment of Aγ is happening due to the creation of a new area between the solute cluster and the matrix. The size difference between solute atoms and the matrix which creates the volume strain and increment of free energy is occurred by VΔGs. Then total free energy ΔG can be illustrated as,

$$\Delta G = -V\Delta G_{v.} + A\gamma + V\Delta G_s \qquad (1)$$

For the sake of understanding, assume the solute cluster is in spherical [7][6], then above eq (1) can be re-written as,

$$\Delta G = -\frac{4}{3}\pi r^3 (\Delta G_v - \Delta G_s) + 4\pi r^2 \gamma \qquad (2)$$

By differentiating the above eq (2) concerning r, and taking the result as equal to zero, (maximum is zero in mathematically) to calculate the $r_{critical}$ as,

$$r_{critical} = 2\gamma / (\Delta G_v - \Delta G_s) \qquad (3)$$

Considering equation 2 & 3,

$$\Delta G_{critical} = 16\pi\gamma^3 / 3 (\Delta G_v - \Delta G_s)^2 \qquad (4)$$

This phenomenon can be illustrated as shown in Fig 2-1 below.

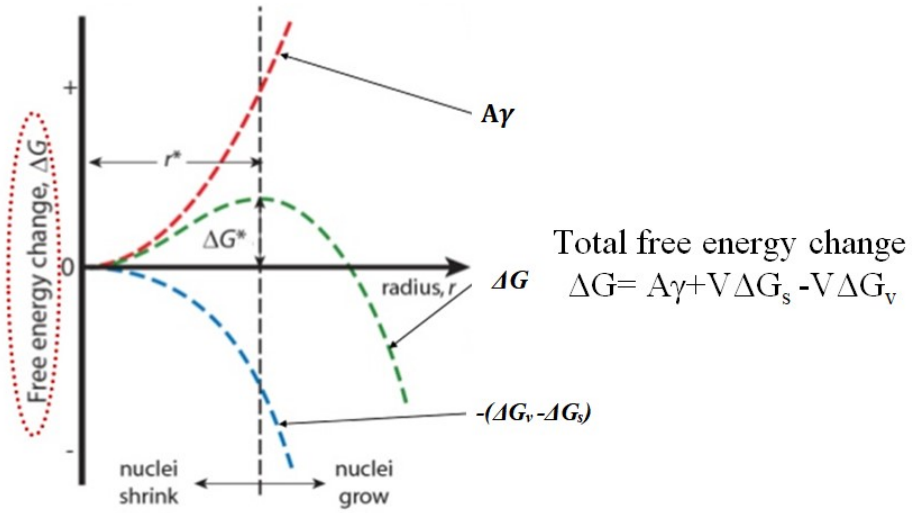

Figure 2-3: Nucleation of a solute cluster

Figure 2-3 shows that, in the beginning, both free energy and the radius of the cluster are increased. At the maximum free energy level, the cluster radius is called $r_{critical}$ and further increment of the radius would reduce the total free energy in the system. This maximum energy level is named as $G_{critical}$ and represents the energy barrier that should overcome for stable cluster formation.

- ❖ Critical radius ($r_{critical}$) is proportionate to the interfacial energy. (see eq.3) This means a critical radius for the solute cluster in the coherent interface (low energy) is comparatively smaller than the incoherent interface.
- ❖ When strain energy (ΔG_s) is increased, $\Delta G_{critical}$ is increased according to the equation (4), same behavior is accounted for the critical radius in nucleation.

This proves that solute atoms would favor reaching cluster larger than the critical size for the stability in a system containing fully coherent atoms. This may prove that the driving force for precipitation is depending on the level of supersaturation. In the end, only large precipitates will remain with small supersaturations.

As time is increased at a given temperature, larger clusters continue to grow and coarsened creating a decreased solute concentration in the aluminum matrix. This coarsening reaction is controlled by the diffusion rate of solute atoms from the aluminum matrix. Simultaneously, tiny and unstable clusters are dissolved and feed solute atoms into the aluminum matrix, which helps further the growth of the larger precipitates. The average size of the precipitate is increased with total number reduction.

2.3 Precipitate Identification by SEM/EDS Analysis

Musa Y. et al find the effect of Mg content on the microstructure and mechanical properties of Al 6063 alloy/Al-Si-Mg alloys. They proved that heat-treated metal contains iron-rich intermetallic compounds such as Al_5FeSi, and $Al_9FeMg_3Si_5$ [26]. A. M. Kilauga et al. [27] had proved that small precipitate colonies such as $Al_{15}(Mn, Fe)_3Si_2$ or $Al_8Mg_3Mg3FeSi6$ were formed due to aging treatment. Those results proved that intermetallic compounds that were formed are iron-rich and Mg-rich, etc.

2.4 Precipitate Size Range

The sequence of precipitate formation with different size ranges which effecting the mechanical properties of the final product would be defined as R_x (x-1,2,3). This can be summarized as below [28].

GP zones → β" needles → β' rods → β Platelets (Mg_2Si) [24] where GP is Guinier Preston

R_1 R_2 R_3

As a result of the continuous nucleation process, several metastable states occurred until the most stable form of Mg_2Si occur. Each metastable form comprises different sizes that would act as obstacles to the dislocation movement in different ways. In this research, the different size ranges were introduced for the precipitates, considering the available publications and research works that were done by others [3][10][11] [24].

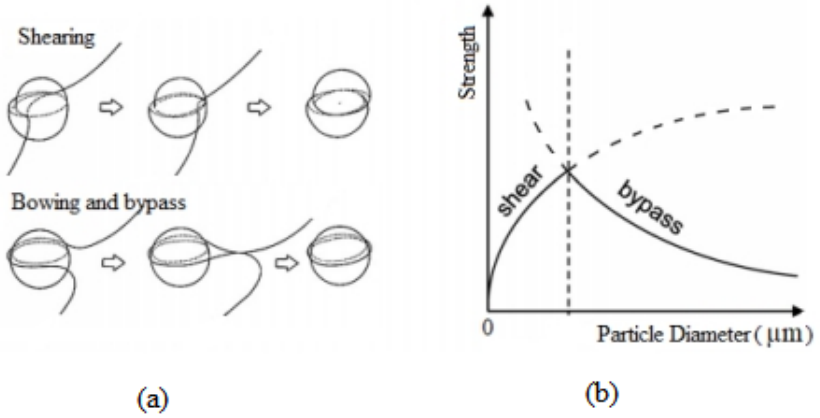

Figure 2-4: Precipitate Size Effect for the Hardening Mechanisms

The degree of strengthening is determined by the particle size, size distribution as well as inter-particle spacing. In this work, all types of precipitates distributed in the matrix (solid solution) are considered the second phase and denoted as β. Several research reports [3][10][11] have shown that the "cutting through" (shearing) mechanism becomes predominant with the higher percentage of particles in the size range of R_1 (<0.2 μm), and the "bowing and bypassing" mechanism becomes predominant within the particle size range of R_2(0.2-1.5 μm). Further, they have shown that both mechanisms could be activated within the range of R_2 (0.2-1.5 μm) especially the "cutting through" mechanism is activated with the particles closer to 0.2 μm. Precipitates bigger than 1.5 μm (R_3) lead to deterioration of hardness and strength possibly due to the over ageing, which is, coarsening of precipitates/particles beyond a specific limit, absorbing dissolved small precipitates. These coarsened particles result in developing highly stressed areas in the particle-matrix interface.

2.5 Hardening Mechanism

The precipitates formed within the matrix act as obstacles to the dislocation movement and cause hardening in the age-hardening process.

2.5.1 Cutting Through Mechanism

The dislocations are dealing with precipitates in two ways. At the beginning of the precipitate formation, very small and coherent precipitates are simply "cut," as shown in figure 2-5.

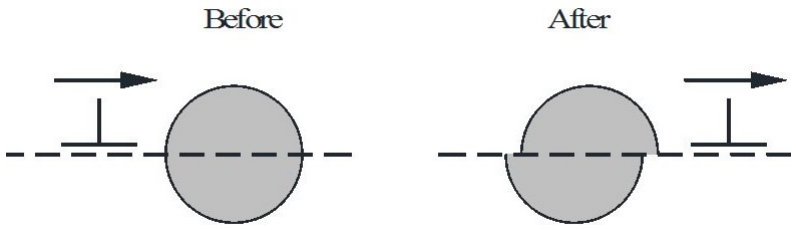

Figure 2-5: Cutting through [29]

As shown above, a precipitate may cut by dislocation, and a more precipitate-matrix interface is created. The upper part of the precipitate is sheared by 'b' called burger vector concerning the lower part at the dislocation entry. A similar operation has happened at the exit of the particle. The creation of a new matrix-precipitate surface area increases the surface energy by $2\pi rb\gamma s$ where γs is the surface energy and r is the particles radius. Then, additional shear stress is needed to deform the particle.

The stress that needs to cut the precipitate is increased continuously with the precipitate size up to a certain level; beyond this level cutting through mechanism cannot be activated.

2.5.2 Bowing and Bypassing

The stress should be increased linearly, as seen in Figure 2-5 if the only hardening mechanism is cutting through. Nevertheless, for bigger precipitates, the bowing and bypass mechanism becomes prominent, and hardness is dropped.

Age hardening is a well-known process that can enhance the mechanical property due to the formation of secondary phase particles within the alloy matrix [17]. Many

experiments/ research has been conducted by many experts due to the importance of this process in the industry. The change in mechanical properties was studied by changing the process parameters, and attempts have been made to improve them further.

An intensive literature survey has been done to summarize the available knowledge, process parameters, and precipitates to determine the boundaries of the proposed work.

2.6. Measure the Hardness.

This testing method consists of indenting the test materials with a diamond indenter of a right pyramid with a square base and a 136^0 angle between opposite faces. Two diagonals of the indentations were left on the metal surface after removing the load as shown in Figure 2-6.

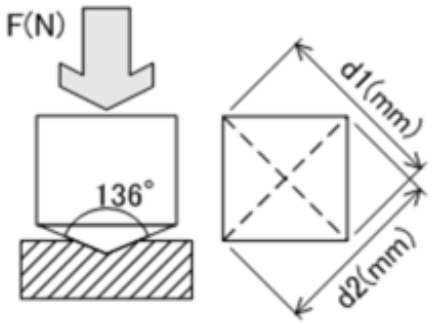

Figure 2-6: Vickers Principle

Dimensions were measured using the microscope and the average was calculated.

$$d = (d_1 + d_2)/2 \text{ ..... (1)}$$

Substituting the average of diagonals, the Vickers hardness was calculated using the eq 2.

$$\text{HV}=\frac{F}{S} = \frac{2F\sin(\emptyset/2)}{d^2} \text{ ..... (2)}$$

Where HV: Vickers hardness

F: Test load (kgf)

S: Surface area of indentation

d: mean value of the diagonals of the indentations (mm)

Φ: the angle between the opposite faces at the vertex of the diamond indenter

$$HV = 1.854 \text{ X } F/d_2 \ldots\ldots\ldots\ldots\ldots (3)$$

Average Vickers Hardness of each sample was calculated using ten numbers from different places. Vickers Hardness can also be calculated using eq. 3 but it is more convenient to use a conversion table which is faster and more accurate. The more accurate and precise value for hardness can be obtained by this method with the same indenter being used for all types of the surface while only changing the force used for the process.

2.7 Image J

This is a Java-based image processing program which can read, display, edit and analyze the SEM image to calculate its size and other details.

CHAPTER 03

3. METHODOLOGY

3.1 Materials and Apparatus

- Al 6063 alloy
- Spark Emission Spectrometer
- Vickers hardness machine
- Power saw & ISOMET Cutting (Silicon carbite saw +Oil)
- Grinding Machine (Silicon carbite papers-600 &1200 grit sizes)
- Distilled water
- Polisher (Water & 1µm diamond suspension)
- Etchant (Keller)
- Scanning Electron Microscope

3.2 Assuring the Chemical Composition of Sample

Al 6063 Alloy, which was homogenized at 570^0C for 2.5 hours were received from Alumex (Pvt) Ltd. The quantitative determination of the alloying elements was tested at three places using Spark Emission Spectroscopy and the elemental percentages were averaged to obtain the result.

3.3 Sample Preparation for Heat Treatment

Disk shape (1cm thickness) metal pieces were cut by the power saw. Continuous coolant supply while cutting was maintained to keep the metal disk at low temperature as much as possible. The final shape was made using a hand saw is shown in Figure 3-1.

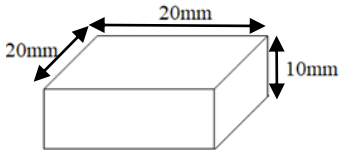

Figure 3-1: Sample for heat treatment

Table 3-1: List of Sample

Sample Name	1	2	3	4	5
Aging Time (minutes)	135	180	225	270	315

The aging time was varied [35][36][37] as shown in table 3-1, while keeping all other factors at constant. Samples were named as listed below by embossing for the identification after treatments.

3.4 Solution Heat Treatment

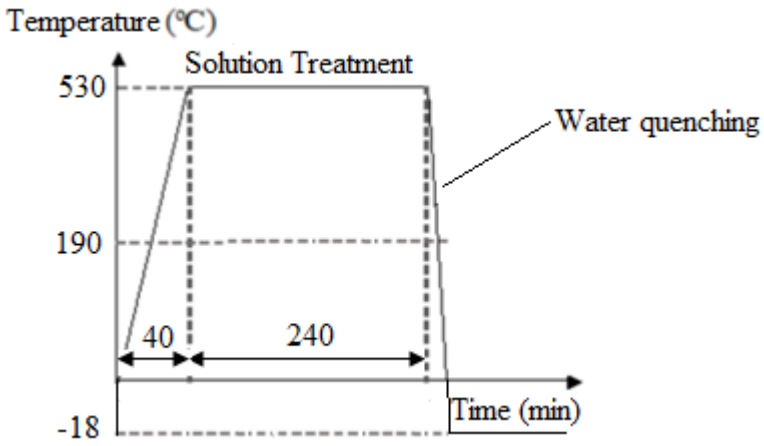

Figure 3-2: Schematic Presentation of Solution Heat Treatment, Firing Profile

The treatment cycle was programmed as illustrated above in Figure 3-2. First 40minutes, the heating rate was 12.5^0C/min and the samples were kept at 530 degrees (temperature) for 240 minutes. Then all samples were quenched in normal water and immediately stored in a deep freezer (-18^0C).

3.5 Aging Treatment

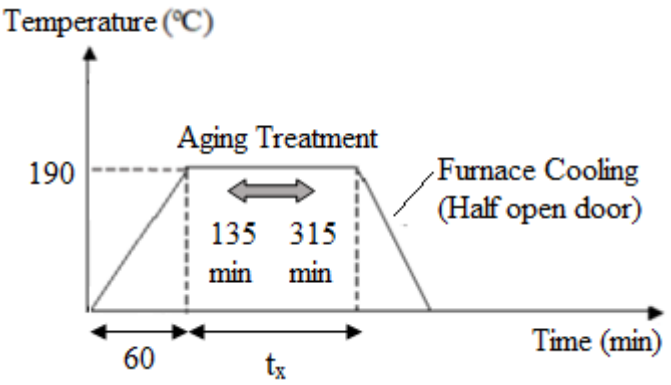

Figure 3-3: Schematic Presentation of Artificial Age-Hardening Treatment, Firing Profiles

The furnace was programmed for the aging treatment using the parameters as mentioned in Figure 3-3. Ageing temperature of 190^0C could reach under the rate of 2.67 ^{0}C/min. This part of the heating profile was the same for all samples (2 pieces/set) while maintaining different soaking times in each heating profile. Treated pieces were cooled within the furnace with the loose door.

Figure 3-4: Programmable Furnace

Both heat treatment processes for all samples were done in the above programmable furnace (Figure 3-4).

3.6 Measure the Hardness.

The heat-treated samples were cut by ISOMET Low speed saw to make a suitable size of 10 mm ×10 mm ×10 mm for the SEM sample holder. Hardness was measured using that cutting surface by applying 5kgf, according to ASTM E92 [19] for 10 seconds at room temperature.

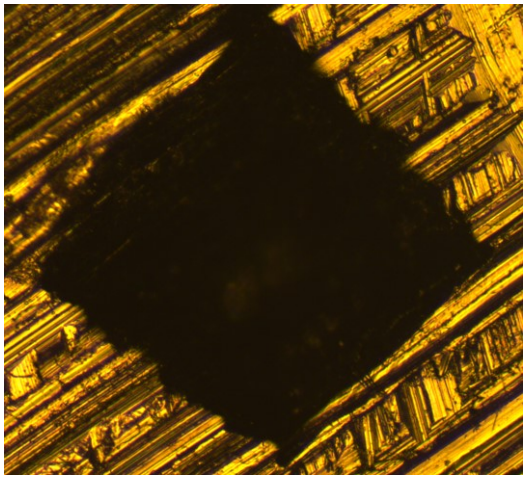

Figure 3-5: Indenting mark on Al 6063 Alloy aged for 180 minutes

3.7. Experimental Procedure-SEM/EDS Analysis

In this work, there are three methods were used for sample preparation for the SEM analysis, and the best method was selected after the SEM observation of surface morphology and SEM/EDS analysis. Furthermore, EDS elemental line, elemental point profiles and SEM vector profiles were obtained for the segments comprising precipitate/β phase and matrix.

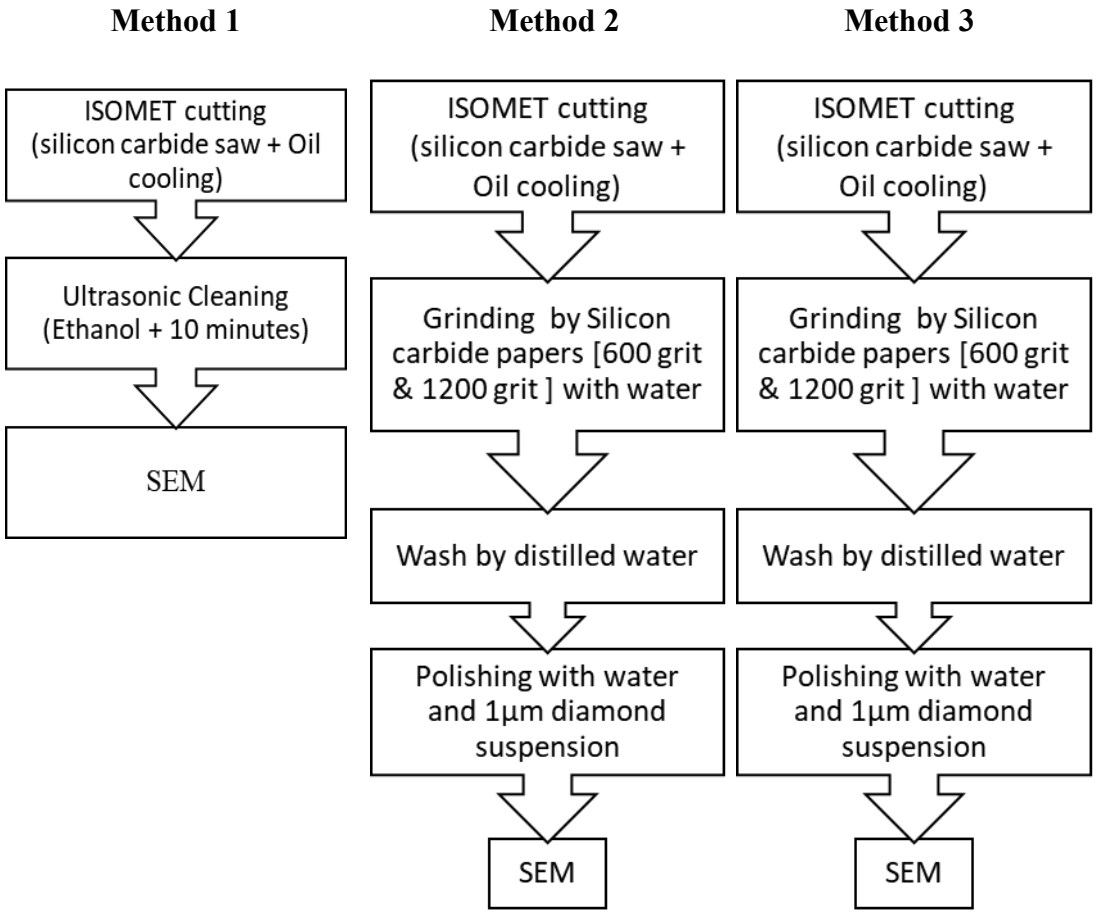

Figure 3-6: Three methods used for Sample preparation.

The specimens were cut by ISOMET at low-speed precision cutting using a well-cleaned silicon carbide saw applying oil as a coolant. The sample surface preparation methods applied before SEM analysis were briefly summarized as follows.

Method 1: The specimen was cleaned using the ultrasonic cleaner with Ethanol and dried by hot air (cutting surface was taken for observation without subjected to grinding, polishing and etching).

Method 2: The specimens were mechanically ground with 600 (10µm-8µm) and 1200 (4µm-3µm) grit silicon carbide papers using water and subsequently polished by universal polisher using 1µm polycrystalline diamond suspension. The specimens were thoroughly washed by distilled water and dried with hot air.

Method 3: Same metallographic processes were applied as method 2,then etched with the Keller solution - 95ml H_2O, 2.5ml HNO_3 ,1.5ml HCl and 1ml HF, for 15 Sec. [26]. Specimens were washed by distilled water and dried with hot air.

3.8 SEM/EDS analysis

The surfaces prepared by all three methods were exposed the four studying has explained below.

1. SEM image capturing.

The captured images should represent the graphical characterization of precipitate size distribution. Ten different areas were selected randomly from one specimen. As a result, around 40 images were taken for one aging time to identify precipitate size distribution formed due to artificial aging.

Here is the parameters of SEM had used.

- Mode: BSD
- Magnification: 5000
- Current: 100μA
- EHT-20 KV

SEM images were taken and read by Image J software. Precipitates were analyzed and calculated the quantity (percentages) belongs to the different size ranges.

2. SEM/EDS elemental point profile for identification of precipitate type

The point profile was done for randomly selected precipitates. Here EDS results were gathered both on the precipitate and matrix near it.

3. Preparation of the line mapping of considering few precipitates.
4. SEM Vector profile for the sample prepared by method 3. [10][15][21]

3.9 Data analysis by IMAGE J Software

40 SEM images were captured belong one aging time (surface quality as method 1) and read those by Image J software. The step by step in software reading has mentioned below.

Step 1: Calibration

The pixel size of the image was calibrated using a known distance and the unit length.

Step 2: Area Separation (duplicate)

Precipitate details such as area and quantity should gather concerning the same area for the sake of comparison.

A rectangle shape of 50 μm X 30 μm (1500 μm^2) was selected as the area for every SEM image. The quantity variation of the number, average size, and the covered area fraction of precipitates due to artificial aging which belongs to the equivalent area are preferred for comparison.

Step 3: Threshold

The threshold was taken for each image using brightness and contrast functions. Particles were displayed clearly on the matrix due to brightness difference.

Step 4: Analysis of Particles

The threshold image was used for analyzed the precipitates. The required data of precipitates such as population, average size, and area fraction (the precipitate utilization percentage) were taken under summarized results. The individual size of each precipitate in one image came out as its results.

Step 5: Calculations

All the below calculations were done assuming the shape of all precipitates are in spherical.

- The average number of precipitates formed in 1500μm^2 area

$$= \frac{\text{Total number of precipitates}}{\text{Number of images}} \quad \ldots\ldots\ldots \quad (1)$$

- The average size of the precipitate

$$= \frac{\text{Sum of average sizes}}{\text{Number of images}} \quad \ldots\ldots\ldots\ldots\ldots\ldots \quad (2)$$

- Area fraction which covered by precipitates

  = Sum of Area fraction…….. (3)

  Number of images

- Percentage of R_1, R_2, R_3

Percentage of precipitates that belong to different size ranges R_1 (< 0.2μm), R_2 (0.2-1.5μm), and R_3 (>1.5μm) were calculated using the cumulative curve of the precipitate radius by curve fitting method [30].

CHAPTER 04

4. RESULTS AND DISCUSSION

4.1 Chemical Composition of Al 6063 Alloy

Table 4-1: Chemical Analysis of Al 6063 Alloy

Element	Si	Mg	Fe	Cu	Mn	Other Minor Element	Al
Wt. %	0.42	0.47	0.53	0.01	0.02	0.25	98.3

The outcome of the spark emission spectrometer has shown above in Table 4-1. The weight percentages of major alloy elements belong to the standard range, proving that materials are suitable for the experimentations.

4.2. Conclude the Surface Preparation Method.

Samples that were homogenized at 570^{o}C for 2.5 hours were received from Alumex (Pvt) Ltd. The samples with 20 mm X 20 mm X 10 mm were prepared using a power saw and hand saw while using proper coolant to prevent microstructural changes. The thermal treatments were arranged as solution treatment at 530^{0}C for 4 hours, followed by age hardening at 190^{0}C for 135,180, 225, 270 and 315 minutes.

Surface preparation suit for SEM analysis was very critical. As explained under methodology, three preparation methods were applied for the sample aged at 190^{o}C for 180 minutes and applied the required tests. The best method was selected after SEM observation of the surface morphology and SEM/EDS analysis for all three methods. Furthermore, EDS elemental line and point profiles and SEM vector profiles were obtained for the segments comprising precipitate/β phase and matrix.

4.2.1 SEM Image Capturing.

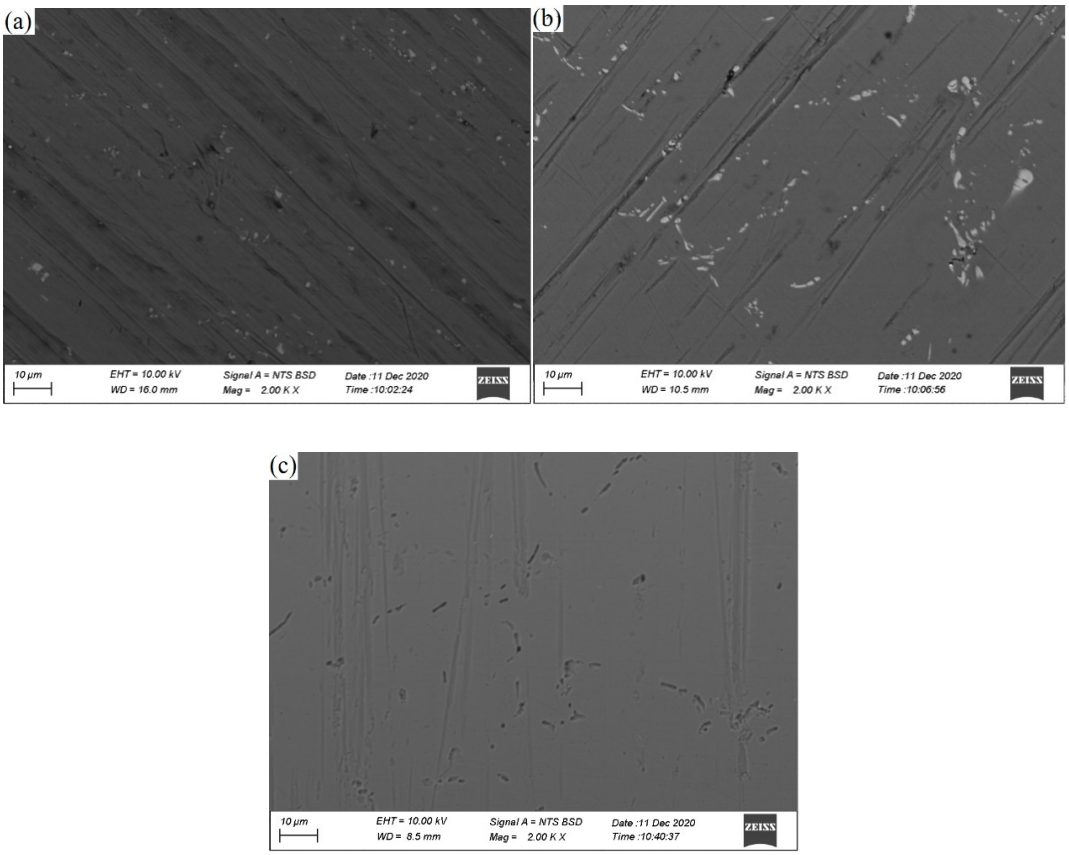

Figure 4-1:Scanning electron micrographs (x 2000) of Al 6063 -T6 aged at 190^{o}C for 180 min: (a) Method 1: (b) Method 2: (c) Method 3

According to the surface morphology shown in Fig 4-1(a) and (b), It is obvious that after applying the grinding and polishing to the initial cutting surface, some precipitated embedded with the surface matrix were well exposed. It seems that most of these precipitates were formed along the α (solid solution of Al, Si, Mg and Fe) grain boundaries. According to Figure 4-1(c), all the precipitates showed in Figure 4-1(b) was dissolved during the etching with Keller solution, and those points were visible as micro pits [31].

4.2.2 SEM Vector Profile

SEM Vector profile is taken for the micro pit areas as shown in Fig 4-2., further justified that these are micro pits. This observation further clarified that the white colour precipitate (it seems like particles) is embedded on the surface matrix.

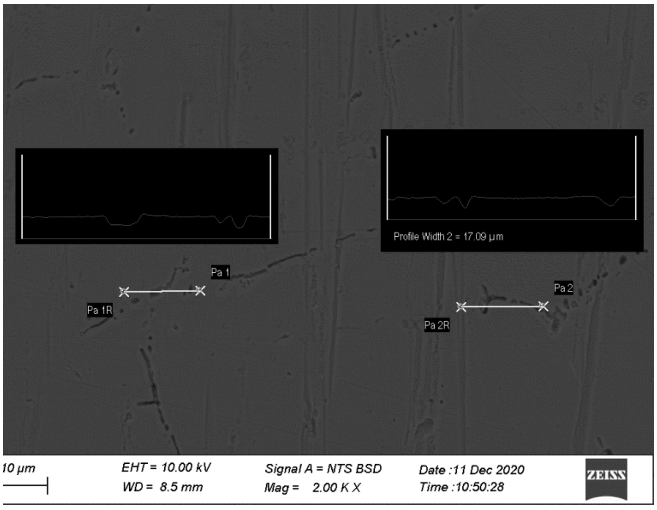

Figure 4-2:SEM Vector profile of micro pit areas of sample prepared by Method 3. (x 2000) (Al 6063 -T6 aged at 190ºC for 180 min)

4.2.3. SEM/EDS Elemental Point Profile for Identification of Precipitate Type

- **Method 2**

The objective of this step is to identify the composition of precipitates/β phase.

According to Figure 4-3, the precipitates/ β phase is composed of some Si and Fe contents and Al and Mg. In the same figure, the matrix (α phase) closer to the precipitate composed only Al and Mg (In SEM/EDS analysis, only the predominantly existing elements are indicated). Therefore, this precipitate can be identified as Si-Fe-rich precipitate. Furthermore, it can be assured that no other ways that Si and Fe can be contaminated as impurities during sample preparation. Therefore, these Si and Fe comprised in the precipitates came from the matrix/α phase.

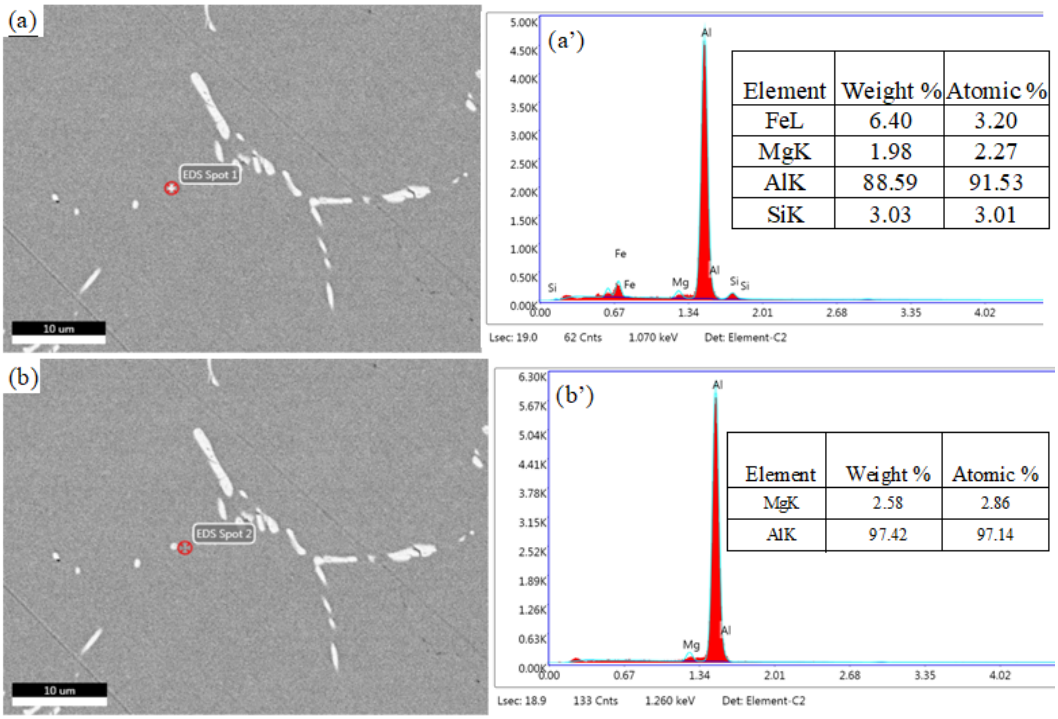

Figure 4-3: SEM/EDS elemental point profile (Method 2): *(a)* on precipitate, (b) in the matrix

- **Method 1**

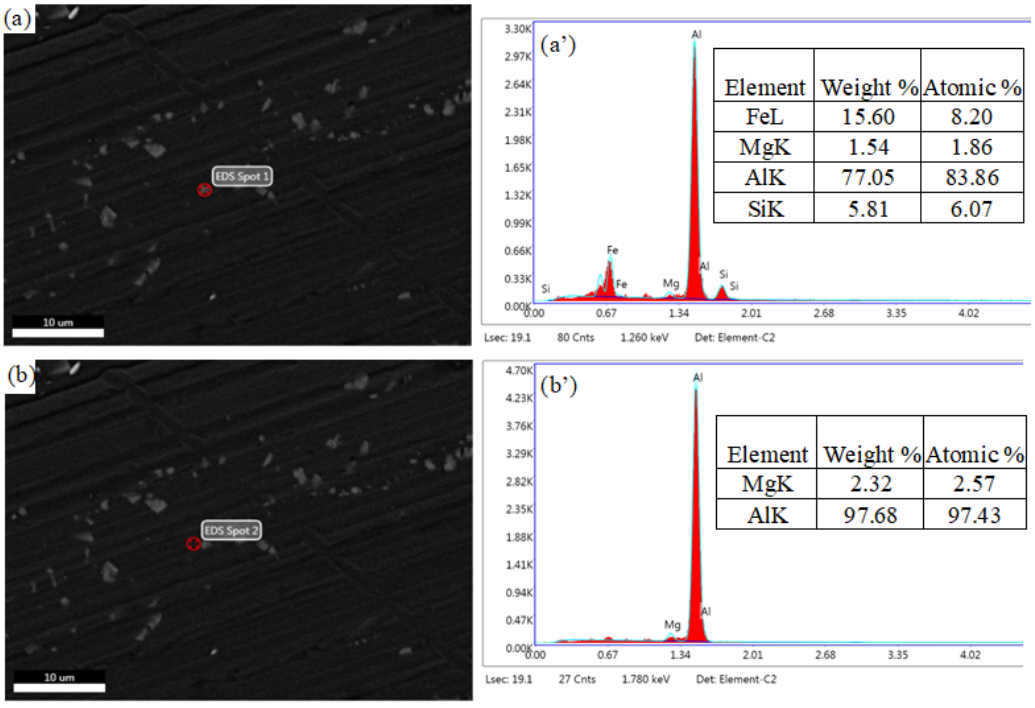

Figure 4-4: SEM/EDS elemental point profile (Method 1): (a) on precipitate, (b) in the matrix.

It is obvious that precipitates shown in Figure 4-4 composed of the same elements-Si and Fe, and both precipitates are Si-Fe-rich precipitate [10][15][21].

4.2.4 SEM/EDS Elemental Line Profile for Identification of Precipitate Type

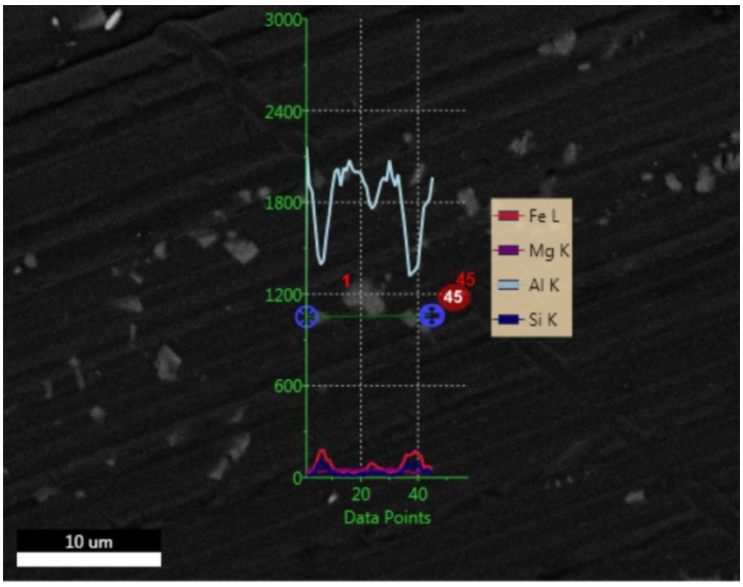

Figure 4-5: SEM/EDS elemental line profile taken across the 3 precipitates and matrix (Method 1)

Figure 4-5 showed the elemental line profile across the matrix and precipitates. This observation of significantly higher positive peaks corresponds to Si and Fe, and negative peaks of Al at the precipitates compared to the matrix, further justified the results obtained in SEM/EDS elemental point profile.

In this work, we focused on samples prepared by Method 1. Those SEM images precipitate sizes and shapes can be appropriately used for the data analysis in Image J Software, for determining particle size distribution [32].

4.3 Precipitate Identification

Surfaces were prepared according to method 1 and enough SEM images were captured. Precipitate identification was made by elemental point profile and elemental line profile for randomly selected precipitates for all different samples. Calculate Silica, Iron and Magnesium weight% comparatively Aluminium on the precipitate and outside of it. Compare the value differently and identified the precipitate/β phase.

Table 4-2: Precipitate/β phase type

Sample name	Type of the β phase
1	Si-Fe-rich
	Si-Fe-rich
2	Si-Fe-rich
	Si-Fe-rich
3	Mg-Si-Fe-rich
	Si-Fe-rich
4	Si-Fe-rich
	Mg-Si-Fe-rich
5	Mg-Si-Fe-rich
	Mg-Si-Fe-rich

As seen in Table 4-2 above, name of two precipitates is included though, there are several precipitates were considered. It is proved that second phase particle types are mixture of Mg, Si and Fe rich.

4.4 Image J Results and Calculations

Enough number of SEM images were investigated by image J software to characterize the precipitate size distribution. Precipitates from the Al matrix are highlighted in the SEM image due to atomic number contrast. During the imaging process, precipitates are properly distinguished from the surrounding matrix by threshold and the number of particles (count), average size. They are a fraction of particles (%) that were measured by software for each image. The results are presented in the summary sheet. The area of each precipitate was considered in the result sheet. Both the summary sheet and results sheet are displayed in Figure 4-6 as an example.

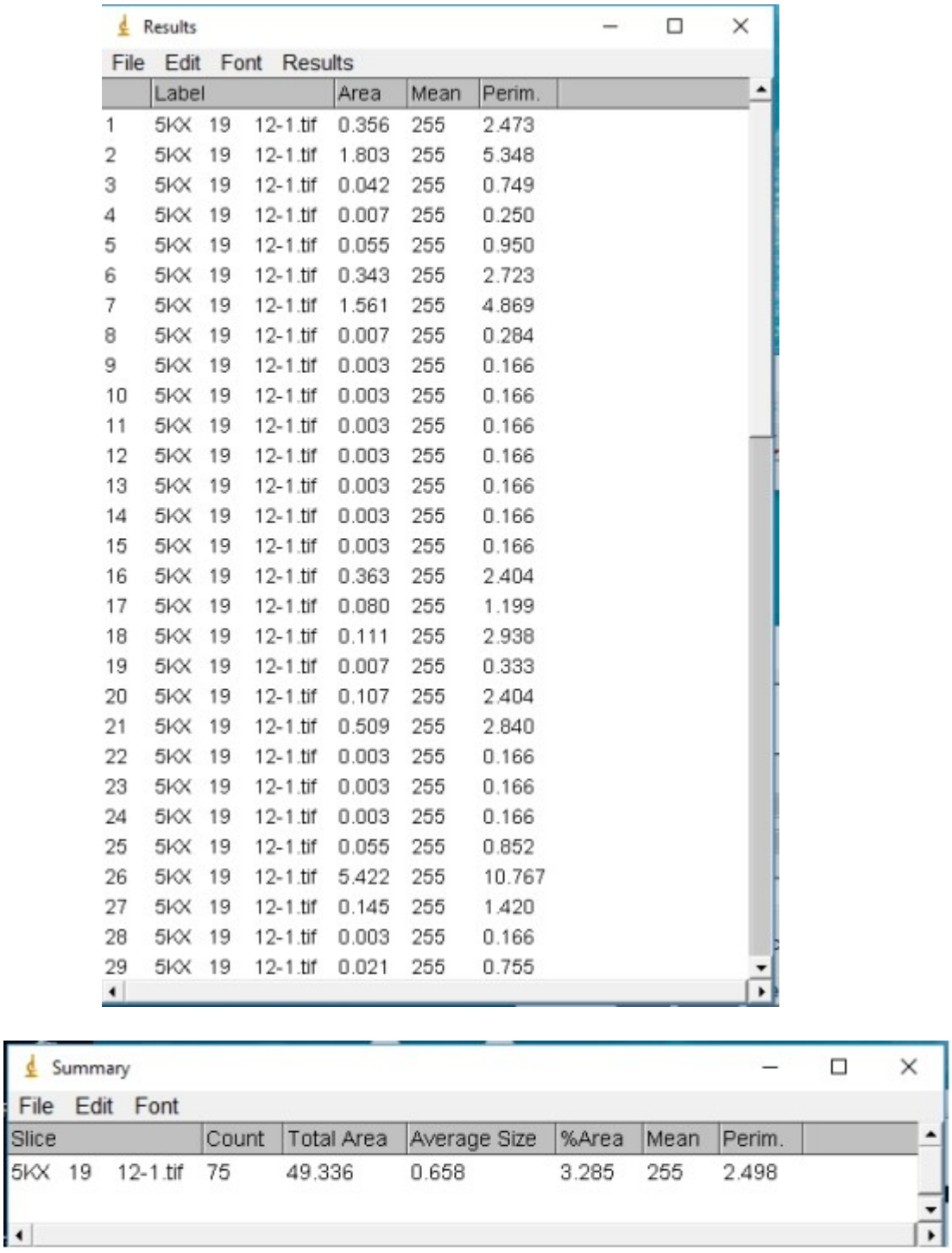

Results

File Edit Font Results

	Label	Area	Mean	Perim.
1	5KX 19 12-1.tif	0.356	255	2.473
2	5KX 19 12-1.tif	1.803	255	5.348
3	5KX 19 12-1.tif	0.042	255	0.749
4	5KX 19 12-1.tif	0.007	255	0.250
5	5KX 19 12-1.tif	0.055	255	0.950
6	5KX 19 12-1.tif	0.343	255	2.723
7	5KX 19 12-1.tif	1.561	255	4.869
8	5KX 19 12-1.tif	0.007	255	0.284
9	5KX 19 12-1.tif	0.003	255	0.166
10	5KX 19 12-1.tif	0.003	255	0.166
11	5KX 19 12-1.tif	0.003	255	0.166
12	5KX 19 12-1.tif	0.003	255	0.166
13	5KX 19 12-1.tif	0.003	255	0.166
14	5KX 19 12-1.tif	0.003	255	0.166
15	5KX 19 12-1.tif	0.003	255	0.166
16	5KX 19 12-1.tif	0.363	255	2.404
17	5KX 19 12-1.tif	0.080	255	1.199
18	5KX 19 12-1.tif	0.111	255	2.938
19	5KX 19 12-1.tif	0.007	255	0.333
20	5KX 19 12-1.tif	0.107	255	2.404
21	5KX 19 12-1.tif	0.509	255	2.840
22	5KX 19 12-1.tif	0.003	255	0.166
23	5KX 19 12-1.tif	0.003	255	0.166
24	5KX 19 12-1.tif	0.003	255	0.166
25	5KX 19 12-1.tif	0.055	255	0.852
26	5KX 19 12-1.tif	5.422	255	10.767
27	5KX 19 12-1.tif	0.145	255	1.420
28	5KX 19 12-1.tif	0.003	255	0.166
29	5KX 19 12-1.tif	0.021	255	0.755

Summary

File Edit Font

Slice	Count	Total Area	Average Size	%Area	Mean	Perim.
5KX 19 12-1.tif	75	49.336	0.658	3.285	255	2.498

Figure 4-6: Out Comes of Image J software (Results) for of Al 6063 alloy, solution treated at 530^{0}C for 4 hours, quenched in water and artificially aged at 190^{0}C for 225 minutes.

4.5 The Influence of Precipitate Size Distribution on Hardness of Aluminium 6063 Alloy

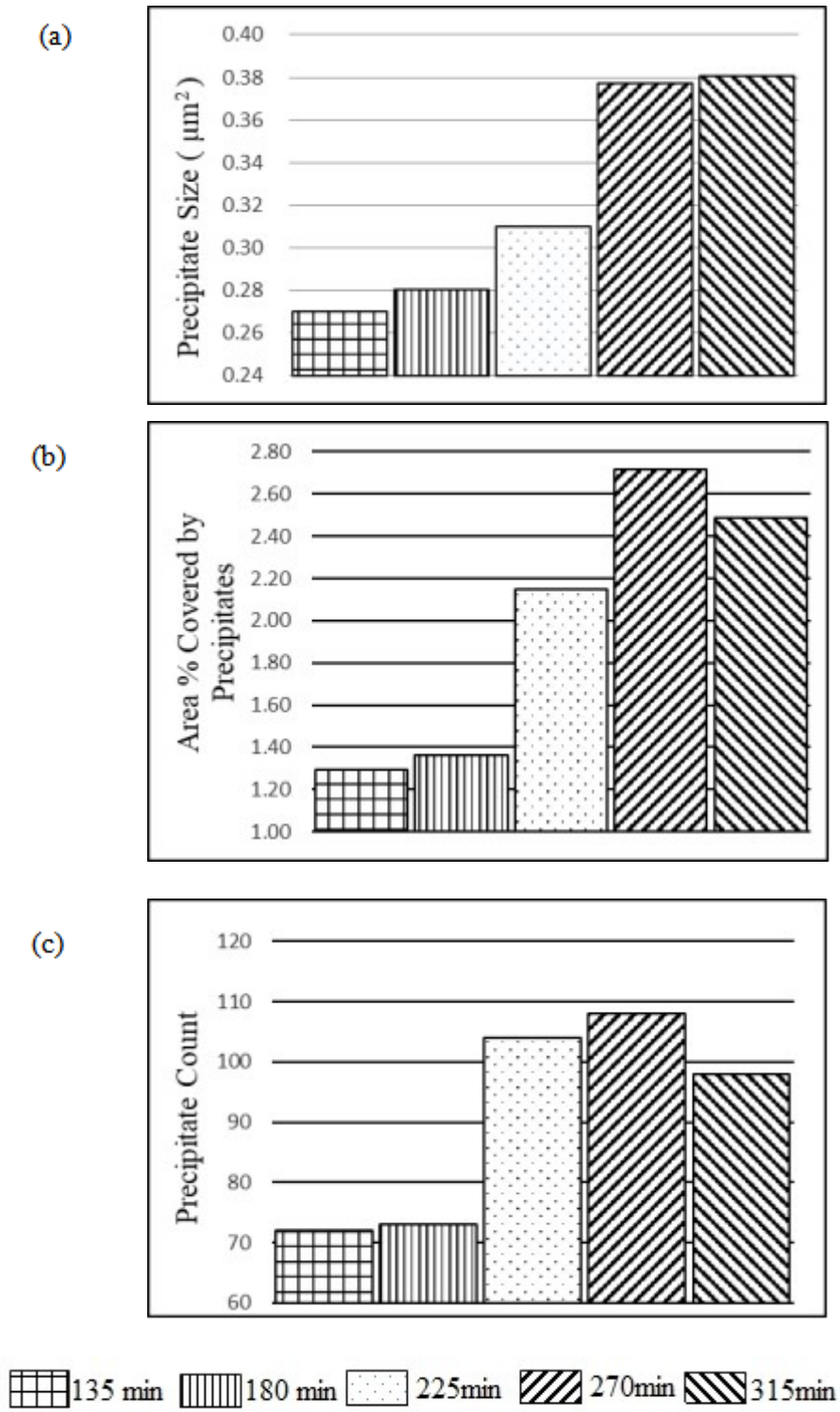

Figure 4-7: Precipitate (a) count (b) Average size and (c) Area fraction for all heating profiles

The calculated results in Figure 4-7 (a), (b) and (c) would give the idea of precipitate formation in all stages [27], growth and further changes that happened during treatments. The formation of precipitates is started with the continued absorption of energy from outside. In the beginning, tiny size and quantity appear. The average number of precipitates was increased slightly at an early stage (135 min to 180 min), but a sudden increment was shown at 225- minutes (180 min to 225 min). The maximum amount of precipitate is recorded at 190^0C for 270 minutes. The same pattern has followed by the area fraction of particles (% area), while the maximum area fraction has recorded at the same place of 190^0C for 270 minutes. At a soaking time of 315 minutes, the reduction of area fraction of precipitate is occurred, while reducing the number of precipitates.

Theoretically, when precipitate reaches its critical radius, it starts to grow continuously while getting solute atoms from dissolving small precipitates. At this point, no more solutes come from the matrix due to the constant volume fraction. If the majority behave like this, the resultant of the system is this nature. However, the average size of the precipitates is increased (Fig.4-7(a)) accordingly. When the behavior of three parameters is combined, this could have possibly happened because of the phenomenon of over ageing while the system absorbed heat continuously.

This is further verified by the hardness variation shown in Table 4-3.

4.5.1 Mechanical Property

The hardness of the samples at different aging times are in below table.

Table 4-3: Vickers Hardness at different aging times

Aging time (minutes)	HV
135 min	99.4
180 min	103.0
225 min	112.9
270 min	143.9
315 min	133.0

According to Table 4-3, the hardness is increased until 270 minutes and then the reduction is started. Simultaneously, the number and area fraction of precipitate reduction occurs while continuous increment has shown in the precipitate size. These results confirmed that coarsening/over the ageing of precipitates by absorbing dissolved meta-stable precipitates around them had reached the critical stage [7]. The variation of the hardness with ageing time has illustrated in Figure 4-8.

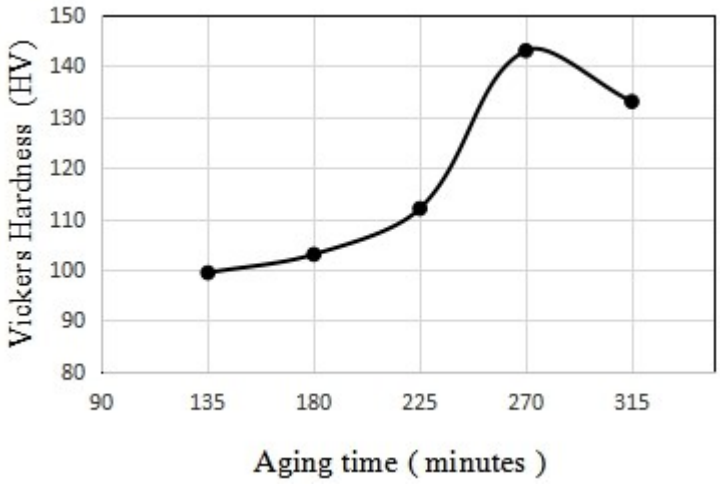

Figure 4-8: Hardness Vs. Aging time

4.6 Relationship Between Hardness Vs. Size Distribution

As explained in chapter 1 and 2, three particle size ranges have been introduced in this research to characterize the precipitate size distribution effect on hardness of the Al 6063 alloy.

Table 4-4: Percentage of Precipitate belongs in different size ranges.

Aging time	0.00-0.2 µm R_1	0.2-1.5 µm R_2	1.5 µm < R_3
135 min	51.0	43.8	5.2
180 min	56.4	38.6	5.0
225 min	66.0	29.5	4.5
270 min	51.5	46.9	1.7
315 min	50.7	42.7	6.6

The results revealed that all particles are less than 3.2 µm in this research. As in Figure 4-8, the particular area of precipitate is gained by Image J, supposing the precipitates are spherical [6]. The number of precipitates which are belonged to different size ranges for different ageing times is concluded as illustrated in Table 4-4. According to the explanation, the alloy gradually gets harder with an increment of ageing time at an elevated temperature of 190^0C. Nucleation, formation and growth of precipitates in Al 6063 alloy has happened and maximum hardness value is achieved by the Al 6063 Alloy, which aged for 270min. Mechanical properties have been changed after that due to over ageing as a result of constant volume fraction. The precipitate size distribution effect on the hardness of Al 6063 Alloy has been considered before ageing because the microstructure behavior is changed.

a) Data Table

Aging time	Precipitate %<1.5µm (R_1+R_2)	Hardness (HV)
135 min	94.8	99.4
180 min	95.0	103
225 min	95.5	112
270 min	98.4	143

b) Graph

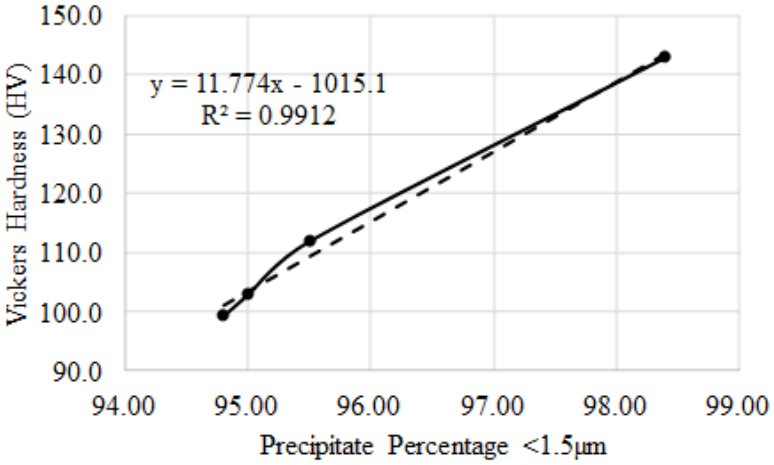

Figure 4-9: Effect of Precipitate Size (< 1.5µm) Distribution on Hardness of Al 6063 Alloy

The results in Figure 4-9 exhibit bi-linear variation between Vickers hardness and precipitate percentage (size less than 1.5 μm) for Al 6063 Alloy. The nature of variation of hardness versus, precipitation percentage indicates considerable deviation of hardness beyond a precipitate quantity possibly due to the change in hardening mechanism of precipitates. The magnitudes of hardness for the different of precipitate percentage have been determined by linear regression analysis.

The mechanisms of getting hardness by precipitates are mainly governed by their size and distance between each other (inter particle distance which I did not use for my calculations). If majority of precipitates belongs to less than 0.2 μm (R1), metal is hardened by cutting through predominant. The precipitates which size is around 1.5 μm (R2) hardened the alloy by predominant of bowing and bypassing. The maximum hardness is occurred for 270 min aged sample, with a huge concentration of smaller precipitates at 225 min (Table 4-4) aging sample.

The meta-stable formation of precipitates (different sizes) in Al 6063 alloy was studied under varying of temperature for constant soaking time as well as varying of soaking time at the same elevated temperature. S.K. Panigrahi and Jayaganthan [33] had found GP zone, β",β' and stable β that were observed for 1 hour soaking in a series of temperature 150^{o}C, 175^{o}C, 200^{o}C and 250^{o}C respectively. Another research group: J Buha et al[34] had done the experiment at 177^{o}C in different soaking times. GP zone for 4 h, β" for 15 h and β' for 160 h accordingly. These literatures are further confirming that different size of precipitates formation at different heating profiles.

A linear relationship between precipitates Vs hardness developed and the linear regression analysis has done as Y= 11.77X – 1015.1. It is worth noting that the relationship has developed for the specific data range and the equation is valid only within this range (data used for graph preparation)

The coefficient of Determination, R^2 is 0.9912 which is closed to 1 is a very good sign for fitness of the graph. The relationship between two variables are more comprehensive. This mean the proportion of the variance in the dependent variable that is predictable from the independent variable.

CHAPTER 05

5. CONCLUSIONS

1. The Si-Fe rich and Mg-Si-Fe-rich were the two types of secondary phase precipitates that were formed at all heating profiles which were revealed by the SEM/EDS examination results.
2. Percentage of precipitates that the particle size less than 1.5 μm (R_1 + R2) was increased to its maximum value of 98.4% at the aging time of 270 minutes while recording the maximum hardness of 143.9 HV.
3. At the aging time of 270 minutes, percentages of precipitates were belonged to three different size ranges were 51.5%, 46.9% and 1.7% for 0.0-0.2μm (R_1), 0.2-1.5 μm (R_2) and above1.5 μm (R_3) respectively.
4. A significant decrease in hardness was evidenced when the particles are coarsening above 1.5 μm, possibly due to the over aging, for the aging time beyond 270 min- at the 315 min, percentage of precipitates above 1.5 μm is 6.6% that is a significant increment relative to the aging time of 135-270 min.
5. The hardness increments due to precipitates which size less than 1.5μm is a function of, $h(x)$=11.774X- 1015.11(for a given precipitate range) with the coefficient of determination, R^2 as 0.9912.

CHAPTER 06

6. SUGGESTION FOR FUTURE WORKS

1. Studying the influence of precipitate size distribution on tensile strength of Al 6063 alloy.
2. Studying the effect of aging temperature on precipitate size distribution and further, their influence on mechanical properties.
3. Developing a model to find the required combination of aging time and temperature to achieve a given combination of hardness and tensile strength.

REFERENCE

[1] F. Ozturk, A. Sisman, S. Toros, S. Kilic, and R. C. Picu, "Influence of aging treatment on mechanical properties of 6061 aluminum alloy," *Mater. Des.*, vol. 31, no. 2, pp. 972–975, 2010.

[2] M. J. Couper, "Selecting the Optimum Mg and Si Content for 6xxx Series Extrusion Alloys," pp. 0–5, 2010.

[3] J. Asensio-Lozano, B. Suárez-Peña, and G. F. V. Voort, "Effect of processing steps on the mechanical properties and surface appearance of 6063 aluminium extruded products," *Materials (Basel).*, vol. 7, no. 6, pp. 4224–4242, 2014.

[4] S. Softening, E. During, and C. O. F. Aluminum, "Modelling of Precipitation and Dissolution of Mg2Si in AlMgSi alloys," pp. 378–385.

[5] G.Al-Marahleh, "Effect of Heat Treatment Parameters on Distribution and Volume Fraction of Mg2Si in the structural Al 6063 Alloy." .

[6] A. J. Kulkarni, K. Krishnamurthy, S. P. Deshmukh, and R. S. Mishra, "Effect of particle size distribution on strength of precipitation-hardened alloys," *J. Mater. Res.*, vol. 19, no. 9, pp. 2765–2773, 2004.

[7] M. H. Jacobs, "1204 Precipitation Hardening," *TALAT Lect.*, 1999.

[8] A. Cuniberti, A. Tolley, M. V. C. Riglos, and R. Giovachini, "Influence of natural aging on the precipitation hardening of an AlMgSi alloy," *Mater. Sci. Eng. A*, vol. 527, no. 20, pp. 5307–5311, 2010.

[9] Z. Guo and W. Sha, "Quantification of Precipitation Hardening and Evolution of Precipitates," *Mater. Trans.*, vol. 43, no. 6, pp. 1273–1282, 2005.

[10] S. J. Lillywhite, P. B. Prangnell, and F. J. Humphreys, "Interactions between precipitation and recrystallisation in an Al–Mg–Si alloy," *Mater. Sci. Technol.*, vol. 16, no. 10, pp. 1112–1120, 2012.

[11] R. Qiang Gao, K. Stiller, V. Hansen, A. Oskarsson, and F. Danoix, "Influence of Aging Conditions on the Microstructure and Tensile Strength of Aluminium alloy 6063," *Mater. Sci. Forum*, vol. 396–402, pp. 1211–1216,

2009.

[12] E. Nembach, “Strengthened Materials : Computer Simulations,” *Acta Mater.*, vol. 49, pp. 2405–2417, 2001.

[13] V. Mohles, D. Rönnpagel, and E. Nembach, “Simulation of dislocation glide in precipitation hardened materials,” *Comput. Mater. Sci.*, vol. 16, no. 1–4, pp. 144–150, 1999.

[14] T. Tadros, “Ostwald Ripening,” *Encycl. Colloid Interface Sci.*, pp. 820–820, 2013.

[15] J. L. Cavazos and R. Colás, “Quench sensitivity of a heat treatable aluminum alloy,” *Mater. Sci. Eng. A*, vol. 363, no. 1–2, pp. 171–178, 2003.

[16] S. Nandy, M. A. Bakkar, and D. Das, “Influence of Ageing on Mechanical Properties of 6063 Al Alloy,” *Mater. Today Proc.*, vol. 2, no. 4–5, pp. 1234–1242, 2015.

[17] Y. Namikawa, K. Sugio, G. Sasaki, J. Tabata, and N. Fuyama, “Relationship between Heat Treatment and Mechanical Properties of Al-Si-Mg Alloy,” *IOP Conf. Ser. Mater. Sci. Eng.*, vol. 547, no. 1, 2019.

[18] W. A. Monteiro, I. M. Espósito, R. B. Ferrari, and S. J. Buso, “Microstructural and Mechanical Characterization after Thermomechanical Treatments in 6063 Aluminum Alloy,” *Mater. Sci. Appl.*, vol. 02, no. 11, pp. 1529–1541, 2011.

[19] A. P. Sekhar, S. Nandy, K. K. Ray, and D. Das, “Prediction of Aging Kinetics and Yield Strength of 6063 Alloy,” *J. Mater. Eng. Perform.*, vol. 28, no. 5, pp. 2764–2778, 2019.

[20] R. A. Siddiqui, H. A. Abdullah, and K. R. Al-Belushi, “Influence of aging parameters on the mechanical properties of 6063 aluminium alloy,” *J. Mater. Process. Technol.*, vol. 102, no. 1, pp. 234–240, 2000.

[21] H. Y. Li, C. T. Zeng, M. S. Han, J. J. Liu, and X. C. Lu, “Time-temperature-property curves for quench sensitivity of 6063 aluminum alloy,” *Trans. Nonferrous Met. Soc. China (English Ed.*, vol. 23, no. 1, pp. 38–45, 2013.

[22] A. Fatai Olufemi, “Ageing Characteristics of Sand Cast Al-Mg-Si (6063) Alloy,” *Int. J. Metall. Eng.*, vol. 1, no. 6, pp. 126–129, 2013.

[23] Y. Namikawa, K. Sugio, G. Sasaki, and J. Tabata, “Relationship Between Heat Treatment And Mechanical Properties Of Al- Si-Mg Alloy Relationship Between Heat Treatment And Mechanical Properties Of Al-Si-Mg Alloy,” 2019.

[24] Smiths Metal Centres Ltd, “Accelerated Ageing in 6xxx series Aluminium Alloys,” pp. 443–450.

[25] M. A. Abdel-Rahman, A. El-Deen, A. El-Nahhas, Y. A. Lotfy, and E. A. Badawi, “Artificial aging behavior of 6063 alloy studied using Vickers hardness and positron annihilation lifetime techniques,” *Defect Diffus. Forum*, vol. 303–304, pp. 31–38, 2010.

[26] M. Yıldırım and D. Özyürek, “The effects of Mg amount on the microstructure and mechanical properties of Al – Si – Mg alloys,” vol. 51, pp. 767–774, 2013.

[27] A. M. Kliauga, E. A. Vieira, and M. Ferrante, “The influence of impurity level and tin addition on the ageing heat treatment of the 356 class alloy,” *Mater. Sci. Eng. A*, vol. 480, no. 1–2, pp. 5–16, 2008.

[28] D. M. Jiang, B. D. Hong, T. C. Lei, D. A. Downham, and G. W. Lorimer, “fracture behaviour of aluminium alloy 6063,” vol. 7, no. November, pp. 1010–1014, 1991.

[29] R. R. Ambriz and D. Jaramillo, “Mechanical Behavior of Precipitation Hardened Aluminum Alloys Welds,” *Light Met. Alloy. Appl.*, no. Figure 1, 2014.

[30] R. Dodampola, S. Amarasingha, D. Attygalle, and S. Weragoda, “Improved method to extract kinetic parameters from thermograms,” *Mater. Today Proc.*, vol.23, Part 1, 2020, pages 2-7.

[31] K. Mizuno, A. Nylund, and I. Olefjord, “Surface reactions during pickling of

an aluminum-magnesium-silicon alloy in phosphoric acid," *Corros. Sci.*, vol. 43, no. 2, pp. 381–396, 2001.

[32] L. Dilrukshi and G. I. P. De Silva, "Effect of Precipitate Size Distribution on Hardness of Aluminium 6063 Alloy," J.Natn.Sci. Foundation Sri Lanka., vol. 48, no. 3, pp. 305-313, 2020.

[33] S. K. Panigrahi and R. Jayaganthan, "Effect of annealing on precipitation, microstructural stability, and mechanical properties of cryorolled Al 6063 alloy," *J. Mater. Sci.*, vol. 45, no. 20, pp. 5624–5636, 2010.

[34] J. Buha, R. N. Lumley, A. G. Crosky, and K. Hono, "Secondary precipitation in an Al-Mg-Si-Cu alloy," *Acta Mater.*, vol. 55, no. 9, pp. 3015–3024, 2007.

[35] G. I. P. De Silva, R. A. D. Perera, and P. V. S. K. Ranasinghe, "Study of the Effects of Two Step Age Hardening Process on Mechanical Properties of Aluminum 6063-T5 Alloy," 19th Annual Symposium, Engineering Research Unit (ERU) , University of Moratuwa, Sri Lanka.,pp. 110–113, 2013.

[36] N.Kodikara and G.I.P.De Silva, " Study of the Effects of Magnesium Content on the Mechanical Properties of Aluminium 6063 Extrudates", Engineer: Journal of the Institution of Engineers,Sri Lanka, Vol: LI, No. 02, pp.1-5, 2018.

[37] G.I.P. De Silva and W.C. Perera, "Improvement of the Mechanical Properties of Aluminum 6063 T5 Extrudates by Varying the Aging Condition Cost-Effectively" South Asian Institute of Technology and Medicine (SAITM) Research Symposium on Advancement of Science, (2012) Sri Lanka.